LASER DRIVEN PARTICLE ACCELERATORS

Francis F. Chen

University of California, Los Angeles, California 90024

I. INTRODUCTION

It is well known that the stimulated Raman scattering instability in laser fusion can produce fast electrons by trapping them in the plasma wave excited by a laser beam. The ω- and k-matching conditions for this parametric instability determine the phase velocity v_ϕ of the wave that would be generated at each density, and hence the energy of the trapped electrons. Such a relation is shown in Fig. 1 for 10.6-μm light. It is seen that at each density two energy groups are possible, the lower energy corresponding to Raman backscatter, and the higher energy to Raman forward scatter; the two energies coincide at the quarter-critical density $n_c/4$, beyond which the Raman instability cannot occur. Two groups of fast electrons, the "hots" and the "superhots," have been seen in computer simulations[1] and in the laboratory[2]; and the variation of energy with density (Fig. 1) has also been verified experimentally[3]. Hyperthermal electrons are undesirable in laser fusion, but their acceleration mechanism can possibly be controlled for use in high-energy physics.

From the standpoint of accelerator designers, electrical breakdown limits the accelerating fields $\underline{E}$ achievable and causes rf linacs to have lengths measured in kilometers. Larger $\underline{E}$ can be obtained at shorter wavelengths; hence the interest in lasers. Of the laser-based schemes proposed, we favor those involving a plasma

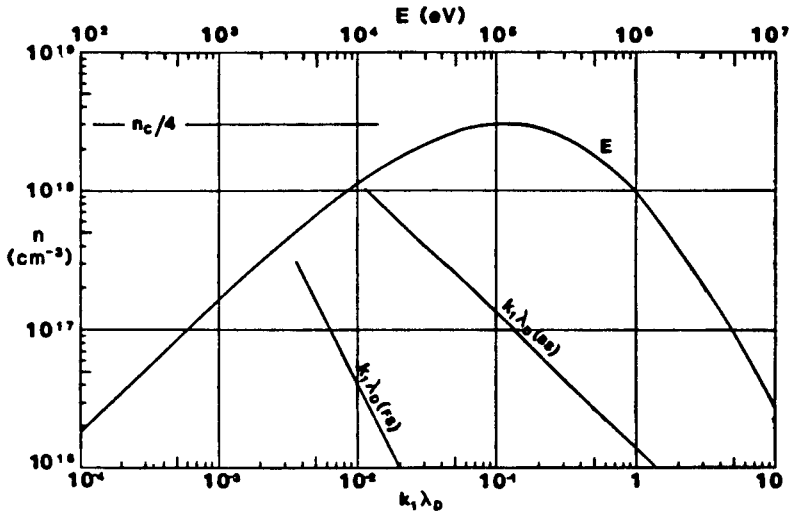

Fig. 1

for three reasons: 1) electric fields of order 1 GeV/cm should be possible in a plasma, compared with < 0.1 MeV/cm (present) to 1 MeV/cm (future) in conventional accelerators, leading to a factor 10^3 reduction in length; 2) there is no breakdown problem, since a plasma is already fully ionized; and 3) there is already experimental evidence that fast electrons can be produced (as shown above) and that plasma waves can be excited by beating laser beams (as will be described later).

In this paper we review the current ideas on two concepts, the Beat-Wave Accelerator (BWA) and the Surfatron, resulting from the work of J. M. Dawson, T. Katsouleas, C. Joshi, and other members of the UCLA group. The main idea is illustrated in Fig. 2. A short laser pulse of length ℓ of order 3 mm (10 psec) is sent into a uniform, underdense plasma and excites an electron plasma

wave of large amplitude. This wave traps bunches of electrons injected near the phase velocity v_ϕ and accelerates them in its large longitudinal E-field. The original idea of Tajima and Dawson[4] assumed the creation of a single soliton with a giant pulse, but we believe that more gentle excitation with the beat-frequency scheme described below will lead to better beam properties. Typically, the length ℓ will contain 30 plasma wavelengths λ_p and 300 laser wavelengths λ_o. Since the group velocity v_g of the light wave turns out to be very close to v_ϕ, the laser pulse, the front of the plasma wave, and the particle trapping and acceleration region move in synchronism through space as fresh plasma waves are created from undisturbed, quiescent plasma. After the light pulse passes, the plasma wave remains because its own group velocity is comparatively small. Ultimately, as the ions begin to move, the plasma wave becomes turbulent due to parametric decay and other processes. The turbulent region is of no consequence because the accelerator action takes place within the length L of coherent waves.

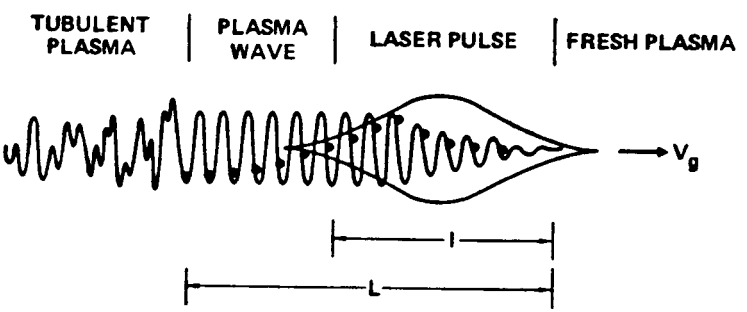

Fig. 2

II. PROPERTIES OF THE PLASMA WAVE

1. Phase velocity. Assume that a plasma wave $(\omega_1, \underline{k}_1)$ is excited by two co-propagating light waves $(\omega_o, \underline{k}_o)$ and $(\omega_2, \underline{k}_2)$ whose beat pattern resonantly drives electron density perturbations by its ponderomotive force. The fastest growing waves follow the matching conditions

$$\Delta\omega \equiv \omega_o - \omega_2 = \omega_1 \simeq \omega_p \tag{1}$$

$$\Delta k \equiv k_o - k_2 = k_1 \equiv k_p \ . \tag{2}$$

Thus

$$v_\phi = \omega_p/k_p = \Delta\omega/\Delta k \ . \tag{3}$$

Since for small $\Delta\omega/\omega_o$ we have $\Delta\omega/\Delta k \simeq d\omega/dk = v_g$, the plasma wave has phase velocity

$$v_\phi \simeq v_g = c(1 - n/n_c)^{\frac{1}{2}} \simeq c \ , \tag{4}$$

where

$$n/n_c \equiv \omega_p^2/\omega_o^2 \ . \tag{5}$$

The process is the same as forward Raman scattering, except that the scattered wave (ω_2, k_2) is in this case injected with the pump (ω_o, k_o). Since $v_\phi \simeq c$, trapped particles can have a large relativistic γ. It is convenient to define γ_ϕ, the γ associated with $\beta_\phi \equiv v_\phi/c$; taking $v_\phi = v_g$, we have

$$\gamma_\phi = (1 - \beta_\phi^2)^{-\frac{1}{2}} = [1 - (1 - n/n_c)]^{-\frac{1}{2}} = (n_c/n)^{\frac{1}{2}} \ .$$

Thus $$\gamma_\phi = (n_c/n)^{1/2} = \omega_o/\omega_p \ . \qquad (6)$$

2. Cold-plasma wavebreaking limit. The maximum amplitude of a plasma wave is limited by wavebreaking, where the electron excursion Δx becomes comparable to $1/k_p$. For $T_e = 0$, the electron equation of motion gives $-m\omega^2\Delta x = ek_p\phi$. Setting $\Delta x = 1/k_p$, $\omega = \omega_p$, and $\omega_p/k_p \simeq c$, we obtain

$$|e\phi_{max}| = m\omega_p^2/k_p^2 = mc^2 \ . \qquad (7)$$

Thus, in a wave at the wavebreaking limit, an electron has potential energy equal to its rest mass.

3. Electric field. The maximum E-field in a plasma wave can be found by setting $\Delta n = n_o$ in Poisson's equation or, equivalently, by multiplying Eq. (7) by k_p/e:

$$E_{max} = \omega_p mc/e = 0.96\ n^{1/2}\ \text{V/cm} \ . \qquad (8)$$

Thus, for $n = 10^{18}\ \text{cm}^{-3}$, eE_{max} is $\simeq 1$ GeV/cm at the wavebreaking limit. For comparison, the E-field of a laser beam (of any wavelength) is

$$E_o = 27\ I_o^{1/2}\ \text{V/cm} \ . \qquad (9)$$

At an intensity I_o of $10^{15}\ \text{W/cm}^2$, Eq. (19) gives $eE_o = 0.85$ GeV/cm. However, this field cannot be used directly because it is perpendicular to $\underline{k}_o$ and Lorentz transforms to 0 in the frame moving with the wave.

4. Saturation by electron trapping. A plasma wave with $v_\phi > v_e = (KT_e/m)^{\frac{1}{2}}$ will trap increasing numbers of electrons from the distribution f(v) as it grows. Since there are more slow electrons than fast ones, this loss of energy eventually stops the wave growth. Numerical studies have shown[5] that the trapping limit is well approximated by a waterbag model where f(v) is flat up to a maximum velocity $v_m = \sqrt{3}\, v_e$. As shown below in Eq. (22), a particle (β,γ) in the lab frame will be trapped if

$$\varepsilon > \gamma(1 - \beta\beta_\phi) - \gamma_\phi^{-1} , \tag{10}$$

where we have defined

$$\varepsilon \equiv e\phi/mc^2 \tag{11}$$

to be the wave amplitude normalized to the cold-plasma wave-breaking limit. Hence, ε_{max} can be estimated by evaluating (β,γ) at $v = v_m$. In a cold plasma, setting $\beta = 0$, $\gamma = 1$ gives

$$\varepsilon_{max} = 1 - \gamma_\phi^{-1} \simeq 1 . \tag{12}$$

Thus, trapping and wavebreaking occur at the same amplitude when $T_e = 0$. In a warm plasma $\beta \ll 1$, the most severe limit occurs when $\beta_\phi \ll 1$. Expanding γ and γ_ϕ as $\gamma \simeq 1 + \beta^2/2$ in Eq. (10) gives $\varepsilon_{max} = \frac{1}{2}(\beta_\phi - \beta)^2$ or

$$e\phi_{max} = \tfrac{1}{2}\, m(v_\phi - v_m)^2 , \tag{13}$$

as expected. For the relativistic waves of interest, we may let $\beta_\phi = 1$, $\beta << 1$ in Eq. (10) to obtain

$$\epsilon_{max} = 1 - \frac{v_m}{c} - \frac{1}{\gamma_\phi} . \qquad (14)$$

Since $v_e << c$, particle trapping does not greatly alter the wave-breaking limit $\epsilon = 1$ as long as γ_ϕ is $>>1$.

III. THE BEAT-WAVE ACCELERATOR

1. Maximum energy gain. In the simplest configuration, a plasma wave (ω_p, k_p) is generated by optical mixing of two laser beams (ω_o, k_o) and (ω_2, k_2), all $\underline{k}$'s being in the $+\hat{x}$ direction. A particle trapped in the wave does not simply have $\gamma = \gamma_\phi$, since it can fall to the bottom of the potential well and be released at that point. A small additional velocity gain in a frame already moving with $\gamma_\phi >> 1$ results in a large energy gain in the lab frame. Let a particle (β,γ) have momentum $p = \gamma\beta Mc$ and energy $W = \gamma Mc^2$ in the lab frame and β', γ', p', W' in the wave frame moving with velocity $v_\phi = \omega_p/k_p$ in the $\hat{x}$ direction and with a corresponding β_ϕ, γ_ϕ. Using the Lorentz transformation

$$\begin{pmatrix} cp \\ iW \end{pmatrix} = \begin{pmatrix} \gamma_\phi & -i\beta_\phi\gamma_\phi \\ i\beta_\phi\gamma_\phi & \gamma_\phi \end{pmatrix} \begin{pmatrix} cp' \\ iW' \end{pmatrix} , \qquad (15)$$

we obtain

$$W = \gamma_\phi \gamma'(1 + \beta_\phi \beta')Mc^2 = \gamma Mc^2 \qquad (16)$$

or

$$\gamma = \gamma_\phi \gamma'(1 + \beta_\phi \beta') \ . \qquad (17)$$

The plasma-wave electric field $\underline{E}$, being parallel to $\underline{v}_\phi$, is not transformed ($E' = E$); but the potential $\phi = iE/k_p$ is transformed to

$$\phi' = \gamma_\phi \phi \qquad (18)$$

since Lorentz contraction gives $k_p' = k_p/\gamma_\phi$.

Consider a particle of charge q and mass M at rest in the wave frame with $\phi' = 0$. A plasma wave grows to an amplitude ϕ' and traps the particle, which falls to the bottom of the potential well, gaining a kinetic energy $|q\phi'|$. Its total energy is $W' = |q\phi'| + Mc^2 = \gamma' Mc^2$. Since $\phi' = \gamma_\phi \phi = \gamma_\phi \varepsilon mc^2$ from Eq. (11), we have (for $|q| = e$)

$$\gamma' = 1 + \varepsilon \gamma_\phi m/M \qquad \beta' = [1 - (1/\gamma'^2)]^{1/2} \ . \qquad (19)$$

Eqs. (16) and (19) give the final energy of the particle in the lab frame. Since its initial energy was $W_o = \gamma_\phi Mc^2$, the energy gain is

$$\Delta W = \gamma_\phi [\gamma' (1 + \beta_\phi \beta') - 1]Mc^2 \ , \qquad (20)$$

with (β', γ') given by Eq. (19). For <u>electrons</u>, we have $M = m$, $\beta' \simeq 1$, and $\beta_\phi \simeq 1$, so that

$$\Delta W \simeq [2(1 + \varepsilon\gamma_\phi) - 1]\gamma_\phi mc^2 \simeq 2\varepsilon\gamma_\phi^2 mc^2 \qquad (21)$$

for large γ_ϕ. For instance, if $\gamma_\phi = \omega_o/\omega_p = 100$ and $\varepsilon = 0.2$, then $\Delta W \simeq 2$ GeV. For ions, however, we have $\gamma' \simeq 1$ and $\beta_\phi \simeq 1$, so that $\Delta W \simeq \beta'\gamma_\phi Mc^2 \ll W_o$. Ions are not accelerated effectively in the BWA because the energy gain is scaled to the electron rest mass.

2. Injection energy. A particle can be trapped even if it is moving in the wave frame as long as its kinetic energy does not exceed $e\phi'$. The trapping condition is, therefore, $e\phi' = \gamma_\phi e\phi = (\gamma' - 1)mc^2$, or $\varepsilon = (\gamma' - 1)\gamma_\phi$. Inverting Eq. (17) (changing the sign of β_ϕ) to obtain γ' in terms of γ, we find

$$\varepsilon = \gamma(1 - \beta\beta_\phi) - \gamma_\phi^{-1} . \qquad (22)$$

This can be solved to give the required injection energy $(\gamma - 1)mc^2$ for a given wave amplitude ε. For instance, if $\gamma_\phi = 100$ and $\varepsilon = 0.2$, the injection energy is 760 keV. When $\gamma_\phi^{-1} \ll 1$ and $\beta_\phi \simeq 1$, Eq. (22) has the approximate solution[6] $\gamma \simeq (1 + \varepsilon^2)2\varepsilon$, which gives 818 keV in this case.

3. Acceleration length. The energy gain in the BWA is $\Delta W \simeq eEL$, where L is the acceleration length. If E is approximated by its maximum value $eE = \varepsilon k_p mc^2$ and ΔW by Eq. (21), ε cancels and we have

$$L = 2\gamma_\phi^2 (c/\omega_o)(\omega_o/\omega_p) .$$

Eq. (16) then gives

$$k_o L = 2\gamma_\phi^3 \quad . \tag{23}$$

Though high energies can be obtained by increasing γ_ϕ, the required accelerator length rapidly becomes impractical.

4. Optical mixing. Though $\epsilon = 1$ is possible in principle, it is difficult to achieve this with laser beams because the decrease in ω_p due to the relativistic mass increase causes a dephasing of the wave relative to the pump waves as ϵ increases. Since a strong pump can change the real and imaginary parts of ω_1, the resulting saturation value of ϵ depends on pump intensity. This effect was predicted and calculated by Rosenbluth and Liu[7] and has been confirmed in computer simulations[8]. According to this theory, the saturation amplitude is given by

$$\epsilon_{sat} = \left(\frac{16}{3}\,\alpha_o\alpha_2\right)^{1/3} \tag{24}$$

and initial growth rate by

$$\frac{d\epsilon}{dt} = \frac{1}{4}\,ck_p\alpha_o\alpha_2 = \frac{1}{4}\,\omega_p\alpha_o\alpha_2 \ , \tag{25}$$

the last step coming from $\omega_p/k_p = c$ [Eqs. (3) and (4)]. Here α_o, α_2 are the normalized peak oscillating velocities in the laser beams:

$$\alpha_o \equiv \frac{v_o}{c} = \frac{eE_o}{m\omega_o c} \quad , \tag{26}$$

and similarly for α_2. The relation to intensity I_o in W/cm^2 and laser wavelength λ_μ in microns is given by

$$\alpha_o^2 = 7.31 \times 10^{-19} I_o \lambda_\mu^2 \quad . \tag{27}$$

Though there is not yet any experimental verification of Eqs. (24) and (25), these provide a relation between ε and $\alpha_o\alpha_2$ which in needed for further computations. In a real experiment, ε_{sat} could be lowered by other mechanisms such as plasma inhomogeneities or raised by, say, a frequency modulation of the laser pulses.

The time τ needed to reach ε can be estimated from Eq. (25):

$$\omega_p \tau \approx 4\varepsilon/\alpha_o\alpha_2 \tag{28}$$

If ε equals ε_{sat}, Eq. (24) yields

$$\omega_p \tau \approx 64/3\varepsilon^2 \qquad \text{or} \qquad \omega_o \tau \approx 64\gamma_\phi/3\varepsilon^2 \quad . \tag{29}$$

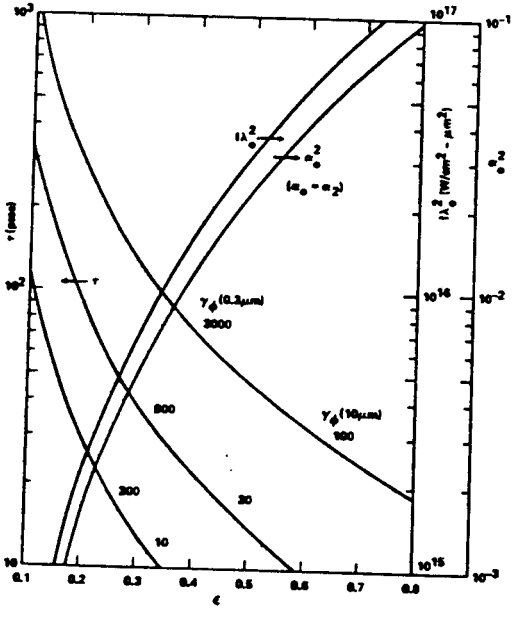

Fig. 3

Fig. 3 shows, for each ε, the value of $I\lambda^2$ needed to reach $\varepsilon = \varepsilon_{sat}$ (if $a_o = a_2$) and the pulselength τ for various combinations of γ_ϕ and λ_o.

5. Pump depletion. Since a plasma wave at the wavebreaking limit contains considerable energy, the length L in Fig. 1 is limited by the energy available in the laser pulse of length ℓ. The energy density in the plasma wave (half field energy and half particle energy) is $k_p^2\phi^2/8\pi$. Since $e\phi = \varepsilon mc^2$ and $k_p = \omega_p/c$, the energy in a length L is

$$W_{epw} = \frac{L}{8\pi}\left(\frac{\varepsilon mc\omega_p}{e}\right)^2 \text{ ergs/cm}^2 . \qquad (30)$$

The energy density in the stronger light wave is $E_o^2/8\pi$. Assuming a square pulse of length ℓ and using Eq. (26), we find

$$W_{laser} = \frac{\ell}{8\pi}\left(\frac{m\omega_o c a_o}{e}\right)^2 \text{ ergs/cm}^2 . \qquad (31)$$

If we define the depletion length L_d by $W_{laser} = 2W_{epw}$, we obtain

$$L_d = \frac{\ell}{2}\left(\frac{\omega_o}{\omega_p}\frac{a_o}{\varepsilon}\right)^2 = \frac{\ell}{2}\frac{\gamma_\phi^2 a_o^2}{\varepsilon^2} . \qquad (32)$$

There is an optimistic result, since the loss energy to the ω_2 beam has been neglected. From the Manley-Rowe relation, we know that (ω_2/ω_p) times as much energy goes into the wave ω_2 as into the plasma wave. However, the ω_2 energy is not entirely lost. By a cascade process, the ω_2 wave continues to feed the plasma wave while decaying successively into waves downshifted by ω_p. Thus we use Eq. (32) to estimate L_d. If, in addition, $\varepsilon = \varepsilon_{sat}$

and $\ell \approx c\tau$, Eqs. (24) and (29) yield

$$k_o L_d = 2\gamma_\phi^3/\varepsilon \ . \qquad (33)$$

Comparing this with the acceleration length L of Eq. (23), we find

$$L/L_d = \varepsilon < 1 \ . \qquad (34)$$

Thus, pump depletion does not seriously affect the BWA, but the maximum energy is limited.

6. Staging. The maximum energy gain can be overcome by constructing the BWA in stages. Two preliminary ideas for separating the particles from the laser beams are shown in Fig. 4. The plasma sources could be theta-pinches, and the density in each would be adjusted to give the proper γ_ϕ, with the previous stage as the injector.

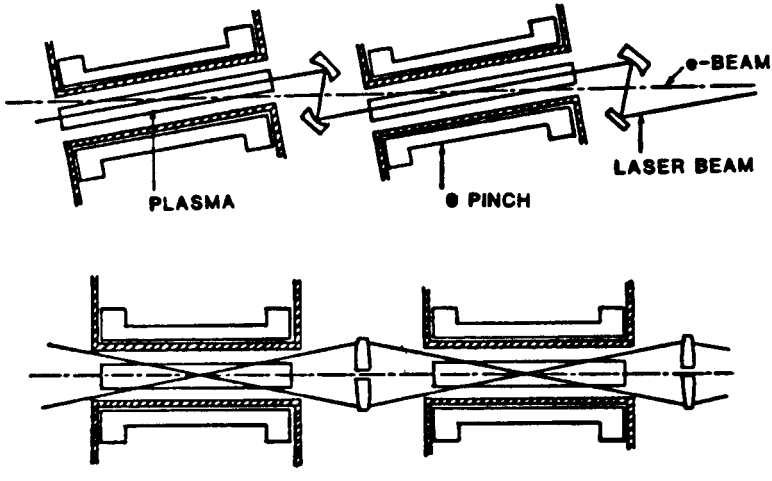

Fig. 4

IV. THE SURFATRON

Since the energy gain in the final stage of the BWA is limited to $\approx\gamma_\phi^2 mc^2$ [Eq. (21)] and $\gamma_\phi^2 \approx n_c/n$ [Eq. (6)], high energy requires low densities, where much of the advantage of high field is lost [Eq. (8)] (unless n_c can be raised by using extremely short wavelength lasers). Fortunately, there is a solution to this problem. In investigating the damping of waves propagating across a magnetic field $\underline{B}$, J. M. Dawson et al.[9] found in computer simulations that such waves were catastrophically damped by a previously unknown mechanism. This mechanism can be used in reverse to accelerate particles in a proposed device called a surfatron[10]. In this scheme, a dc magnetic field $B\hat{z}$ is imposed perpendicular to the plasma wave $k_p\hat{x}$. Particles trapped in the wave and traveling with $v_x \approx v_\phi$ feel a Lorentz force $-qv_xB\hat{y}$ which accelerates them in the $\hat{y}$ direction (Fig. 5). The resulting velocity v_y causes a force component $+qv_yB\hat{x}$ which opposes the accelerating field E_x. When E_x and B have the proper relative magnitude, the particle is prevented from falling to the bottom of the wave's potential trough, as in the BWA. Rather, the particle stays in a stable position near the maximum of E_x and can gain energy indefinitely. Its trajectory is at an angle to the wave fronts; and, in the manner of a surfer on an ocean wave, it can gain a velocity larger than the wave velocity v_ϕ.

1. Non-relativistic motion. For simplicity consider a particle of charge +e in an electric field $\underline{E} = \hat{x}E_o \cos(k_px - \omega_pt)$. The equation of motion $m\dot{v}_y = -ev_xB/c$ with $v_x \approx v_\phi = \omega_p/k_p$ gives

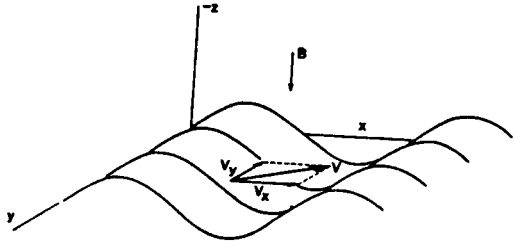

Fig. 5

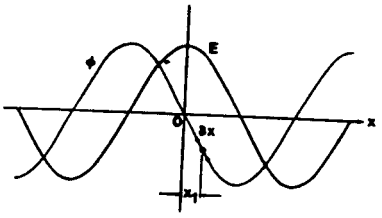

Fig. 6

$$v_y = -\omega_c v_\phi t \ . \qquad (35)$$

The particle is detrapped when $|v_y B/c| > |E_o| = |k_p \phi|$. It then goes into a circular Larmor orbit modulated by the wave. Taking $e\phi \approx \frac{1}{2} m v_\phi^2$ as the amplitude needed to trap particles from rest, we find

$$v_{y\ max} = (\omega_p/2\omega_c) v_\phi \equiv \alpha v_\phi \ . \qquad (36)$$

From Eqs. (35) and (36) it is easily found that the acceleration time, maximum energy, and acceleration distance are given by

$$t = \alpha/\omega_c \ , \quad W_{max} = \alpha^2 \frac{1}{2} m v_\phi^2 \ , \quad L = \alpha^3/k_p \ . \qquad (37)$$

Again there is a trade-off between energy and acceleration distance.

Until the particle is detrapped, it oscillates around an

equilibrium position on the waveform with an amplitude depending on the initial conditions. To show this, let the field and potential in the wave frame be as shown on Fig. 6:

$$\underline{E} = \hat{x}E_o \cos kx , \qquad \phi = -(E_o/k) \sin kx . \tag{38}$$

The equilibrium position x_1 is given by

$$E(x_1) + v_y B/c = 0 , \quad \cos kx_1 = B\omega_c v_\phi t/cE_o , \tag{39}$$

where v_y varies slowly according to Eq. (36). Let $x = x_1 + \delta x$, expand E around x_1, and use Eq. (40):

$$\begin{aligned} \delta\ddot{x} &= (e/m)[E_o \cos k(x_1 + \delta x) + v_y B/c \\ &= (e/m)\, E_o\, (\cos kx_1 - k\delta x \sin kx_1) + v_y B/c \\ &= -(ekE_o/m) \sin kx_1\, \delta x . \end{aligned} \tag{40}$$

This describes an oscillation with frequency given by

$$\omega_b^2 = \omega_{bo}^2 \sin kx_1 , \tag{41}$$

where ω_{bo} is the bounce frequency defined by

$$\omega_{bo}^2 = ekE_o/m . \tag{42}$$

Eqs. (41) and (39) then give

$$\omega_b^2 = \omega_{bo}^2[1 - (B\omega_c\omega t/ckE_o)^2]^{1/2} = [\omega_{bo}^4 - \omega_c^4(\omega t)^2]^{1/2} , \tag{43}$$

showing that ω_b decreases in time. The physical reason is that x_1 moves toward the origin [Eq. (40)], where the restoring force (proportional to dE/dx) is zero. The conservation of action $\oint p_x\,dx$ in this motion shows that $\delta v_x \delta x \propto \omega_b (\delta x)^2$ is constant, so that $\delta v_x \propto \omega_b^{\frac{1}{2}}$. Thus, the oscillation amplitude in velocity space also decreases in time, so that the beam spread is improved over that during injection.

2. Relativistic motion[6]. We first show that detrapping does not occur in the relativistic case for large enough E/B, so that a particle can be accelerated to arbitrarily high energies. The relevant equations of motion are

$$\frac{d}{dt}(\gamma v_x) = \frac{q}{m}\left[E_o \cos(kx - \omega t) + v_y \frac{B}{c}\right] \qquad (44)$$

$$\frac{d}{dt}(\gamma v_y) = -\omega_c v_x \,, \qquad (45)$$

where m and ω_c refer to the rest mass. Since $E_x' = E_x = E_o \sin k'x'$, Eq. (44) in the wave frame is

$$\frac{m}{q}\frac{d}{dt}(\gamma' v_x') = E_o \cos k'x' + v_y' B_z'/c \,. \qquad (46)$$

B_z, being perpendicular to the motion, transforms as

$$B_z' = \gamma_\phi (B_z - \beta_\phi E_y) = \gamma_\phi B_z \,, \qquad (47)$$

since $E_y = 0$. The term $v_y' B_z'/c = v_y' \gamma_\phi B/c$ in Eq. (46) cannot be larger than $E_o \sin k'x'$ if

$$E_o \geq \gamma_\phi B \ , \qquad (48)$$

since $|v_y'| \leq c$. Eq. (48) is the trapping condition; when this is satisfied, there is a steady-state solution in the wave frame where the particle position is given by

$$\cos k'x_1' = \gamma_\phi B/E_o \ . \qquad (49)$$

Depending on the initial conditions, particles can execute damped oscillations about this position as in the non-relativistic case. Here, the damping is even stronger because the relativistic mass increase lowers ω_{bo}.

For a particle held stably at x_1, we have $v_x = v_\phi$. Eq. (45) then gives

$$\gamma v_y = - \omega_c v_\phi t \ , \qquad (50)$$

where $\gamma^2 = (1 - \beta^2)^{-1}$. Thus

$$v_y^2 = \omega_c^2 v_\phi^2 t^2 \left(1 - \frac{v_\phi^2}{c^2} - \frac{v_y^2}{c^2}\right) \qquad (51)$$

Solving for v_y, we have

$$v_y = (-\omega_c v_\phi t/\gamma_\phi)(1 + \omega_c^2 v_\phi^2 t^2/c^2)^{-\frac{1}{2}} \ . \qquad (52)$$

Initially, v_y increases with t; but for $\omega_c t >> c/v_\phi$, v_y approaches the limiting value

$$v_y = c/\gamma_\phi \quad . \tag{53}$$

Since $v_x = v_\phi$, the total velocity is given by $v^2 = v_\phi^2 + c^2/\gamma_\phi^2 = c^2$ in this limit. The surfing angle θ is then given by

$$\theta = \sin^{-1}\theta = v_y/c = \gamma_\phi^{-1} \quad . \tag{54}$$

Fig. 7 shows the orbit of a particle oscillating about x_1 as it is accelerated in the y direction up to the light circle.

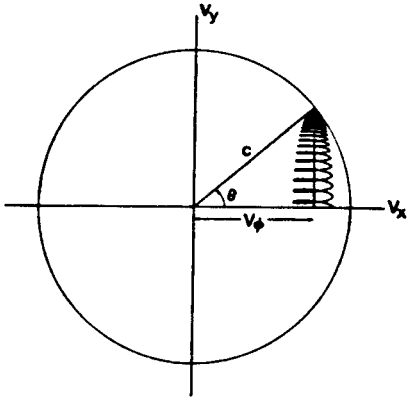

Fig. 7

3. Energy gain. Defining $\tau = \omega_c \beta_\phi t$, we can write Eq. (52) as

$$v_y = dy/dt = -(c/\gamma_\phi)\tau(1+\tau^2)^{-\frac{1}{2}}. \tag{55}$$

For y=0 at t=0, integration gives

$$y(t) = (c^2/\gamma_\phi v_\phi \omega_c)[1-(1+\tau^2)^{\frac{1}{2}}]. \tag{56}$$

Substituting Eq. (53) into Eq. (50), we obtain

$$\gamma(t) = \gamma_\phi(1+\tau^2)^{\frac{1}{2}} \; ; \tag{57}$$

or, in terms of y [Eq. (56)],

$$\gamma(y) = \gamma_\phi\left(\frac{\gamma_\phi v_\phi \omega_c}{c^2}|y| + 1\right) . \tag{58}$$

Since $t = x/v_\phi$ and $\tau = \omega_c x/c$, Eq. (57) can be written

$$\gamma(x) = \gamma_\phi (1 + \omega_c^2 x^2/c^2)^{\frac{1}{2}} . \qquad (59)$$

For colinear beams, as we have assumed so far, Eq. (6) gives $\gamma_\phi = \omega_o/\omega_p$. The spatial energy gain rates are then given by

$$\frac{d\gamma}{dy} = \gamma_\phi^2 v_\phi \omega_c/c^2 \simeq \gamma_\phi \omega_c/c = (n/n_c)(\omega_c/c) \qquad (60)$$

$$\frac{d\gamma}{dx} \simeq \gamma_\phi \omega_c/c = (\omega_o/\omega_p)(\omega_c/c) . \qquad (61)$$

The largest permissible ω_c to be used here is given by Eq. (48). Since $E_o = k_p \phi = \varepsilon k_p mc^2/e$, and $\omega_p \simeq ck_p$, Eq. (48) can be written

$$\omega_{c\ max} = \varepsilon \omega_p/\gamma_\phi . \qquad (62)$$

With this value, Eqs. (60) and (61) are

$$d\gamma/dy = \varepsilon k_p \gamma_\phi , \qquad d\gamma/dx = \varepsilon k_p . \qquad (63)$$

Since $k_p \gamma_\phi = \omega_o/c = k_o$, we finally have

$$\Delta\gamma = \varepsilon k_o \Delta y = \varepsilon k_p \Delta x . \qquad (64)$$

Table I shows the required acceleration lengths Δx and widths Δy for 1 GeV and 1 TeV electron accelerators, assuming $\varepsilon = 0.2$.

TABLE I

	1 GeV	1 TeV
$\Delta\gamma$	2×10^3	2×10^6
ϵ	0.2	0.2
λ_o (μm)	10.6	0.35
$\gamma_\phi = \omega_o/\omega_p = k_o/k_p$	10	30
Δx (cm)	17	1670
Δy (cm)	1.7	56
n (cm^{-3})	10^{17}	10^{19}
B (kG)	20	68
θ (degrees)	5.7	1.9

Once λ_o is prescribed by the laser and γ_ϕ is chosen to reach a compromise between Δx and either n or B, the other quantities are fixed by the preceding equations.

4. How the energy is gained. More insight on the surfatron process is obtained by considering the energy gain mechanism in the laboratory and wave frames. In the wave frame, the particle maintains a stable position on the stationary potential hill but is accelerated along the wavefront by the force $F'_y = qE'_y$. Here E'_y is the field arising from Lorentz transforming B_z from the lab frame: $E'_y = -\gamma_\phi v_x B_z/c = -\gamma_\phi v_\phi B/c$. Hence the particle gains the energy $W' = qE'_y y'$ by moving in the y' direction only. In the lab frame, however, there is an E-field in the x direction only; from this, the particle gains the energy $W = qE_x x$. Though the Lorentz force

$q(\underline{v} \times \underline{B})$ has both x and y components, it cannot give energy to the particle because it is perpendicular to $\underline{v}$. Thus, in the lab frame the particle gains energy only in the x direction, and it is obvious that ions and electrons would gain energy at the same rate.

5. Finite-angle optical mixing. If $\underline{k}_o$, $\underline{k}_2$, and $\underline{k}_p$ are colinear, the laser beams and the plasma wave must be wide enough to cover the excursion Δy of the accelerated particles in the surfatron scheme. From Table I, we see that, even for 1 GeV, Δy is 1.7 cm, considerably wider than the focal diameter of a typical high intensity laser. This problem can be alleviated by arranging for one of the beams to follow the particle trajectory. The geometry and k-matching diagram are shown in Fig. 8. Let $\underline{k}_2$ be an intense, well-focussed beam that travels at an angle θ relative to $\underline{k}_p$, as given by Eq. (54). The plasma wave, which now has wavefronts at an oblique angle to $\underline{k}_2$, can be set up by a wide, weaker beam $\underline{k}_o$ at an angle ϕ relative to $\underline{k}_2$. From Fig. 8, it is seen

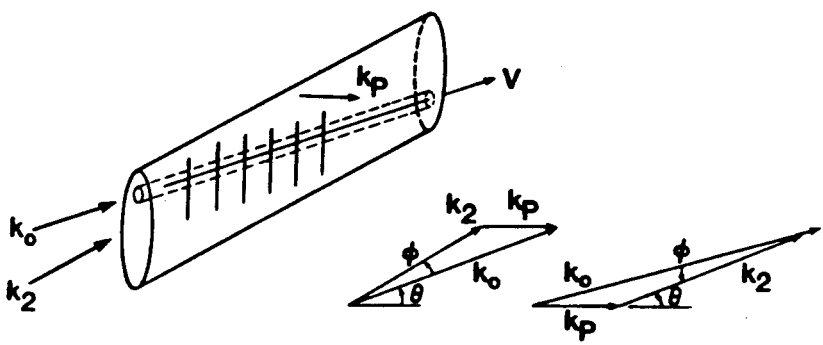

Fig. 8

that the required k-matching to drive the plasma wave can be achieved by choosing ϕ properly when either the bluer beam $\underline{k}_o$ or the redder beam $\underline{k}_2$ is to be the one following the particles. However, the latter case is preferred because it will cause less desynchronization of the article (traveling at $v \simeq c$) with the light pulse (traveling at $v_g < c$). To show this, consider the diagrams of Fig. 9. Let ω_o and ω_p be given; then k_o, k_2, and ω_2 are determined from

$$c^2k_o^2 = \omega_o^2 - \omega_p^2 , \quad c^2k_2^2 = \omega_2^2 - \omega_p^2 , \quad \omega_2 = \omega_o - \omega \quad . \qquad (65)$$

In Fig. 9, particles travel horizontally along $\underline{k}_o$ in (a) and along $\underline{k}_2$ in (b). The colinear k-matching condition is shown at the bottom. As ϕ is varied, the vector $\underline{k}_2$ in (a) and $\underline{k}_o$ in (b) is rotated with its length kept constant. The value of k_p must then increase and v_ϕ decrease relative to the colinear values k_{po} and $v_{\phi o}$. However, particles maintaining the same phase relative to the wave will travel horizontally with velocity $v_{\phi||} = \omega_p/k_p \cos\theta$. It is seen that $k_p \cos\theta > k_{po}$ in Fig. 9(a) and $k_p \cos\theta < k_{po}$ in Fig. 9(b). Thus, $v_{\phi||} < v_{\phi o} = v_g$ and $v_{\phi||} > v_{\phi o} = v_g$, respectively,

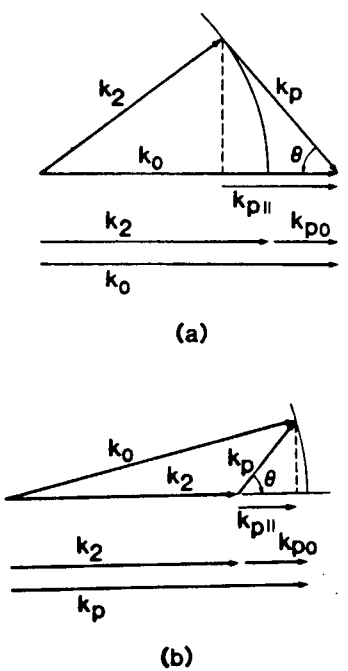

Fig. 9

in these two cases. Since highly relativistic particles have $v_{\phi||} \simeq c$, only case (b) is possible.

We now calculate θ and ϕ from Fig. 9(b). The law of cosines and the law of sines give

$$k_o^2 = k_p^2 + k_2^2 + 2k_p k_2 \cos\theta \tag{66}$$

$$\sin\phi = (k_p/k_o)\sin\theta \ . \tag{67}$$

For particles traveling at c, the surfing angle is given by

$$v_\phi = \omega_p/k_p = c\cos\theta \ . \tag{68}$$

Eliminating θ, k_o, and k_2 from Eq. (66) using Eqs. (65) and (68) and solving for k_p, we obtain for $\beta_\phi = \omega_p/ck_p$:

$$1 + \frac{1}{\beta_\phi^2} = \frac{2\omega_o}{\omega_p}\left[1 - \left(1 - \frac{2\omega_p}{\omega_o}\right)^{1/2}\right] . \tag{69}$$

For small ω_p/ω_o, we expand the square root to second order to obtain

$$\beta_\phi^2 = \left(1 + \frac{\omega_p}{\omega_o}\right)^{-1} , \quad \gamma_\phi^2 = \frac{\omega_o}{\omega_p} + 1 \ . \tag{70}$$

Eq. (68) then gives

$$\cos\theta = \beta_\phi \simeq 1 - \frac{1}{2}\frac{\omega_p}{\omega_o} , \qquad \theta \simeq \left(\frac{\omega_p}{\omega_o}\right)^{1/2} \simeq \frac{1}{\gamma_\phi} \ . \tag{71}$$

Though γ_ϕ is now $\approx (\omega_o/\omega_p)^{\frac{1}{2}}$ instead of ω_o/ω_p as in the colinear case, the relation $\theta \approx 1/\gamma_\phi$ is still valid. The angle ϕ is given by Eqs. (67) and (68):

$$\sin \phi = (\omega_p/\omega_o) \tan \theta , \quad \phi \approx \theta^3. \qquad (72)$$

When the particles have been accelerated to velocity c, they will overtake the laser pulse at the rate

$$c - v_g \approx \tfrac{1}{2}(\omega_p^2/\omega_2^2)c \approx \tfrac{1}{2} (n/n_c)c . \qquad (73)$$

If the acceleration length L (length of the plasma wave) is very long, one would have to inject the particles after the laser pulse, so that the particles will have caught up with the pulse by the time they reach the design value of γ. We shall see, however, that pump depletion limits L to a value such that the velocity mismatch is never a problem.

6. Pump depletion in the surfatron. In optical mixing, each photon of the bluer beam (ω_o) decays into a plasmon and a photon of the redder beam (ω_2). Consequently, only the ω_o beam suffers from pump depletion in the first decay, although the ω_2 beam will also deplete in subsequent steps of the cascade. The depletion length is given by Eq. (32)

$$L_d = \frac{\ell}{2} \frac{\omega_o^2}{\omega_p^2} \frac{\alpha_o^2}{\epsilon^2} , \qquad (74)$$

where we have not identified ω_o/ω_p with γ_ϕ (to allow for off-angle

mixing, where $\omega_o/\omega_p \approx \gamma_\phi^2$). The length ℓ of the laser pulse is given by $\ell = c\tau$, where, without assuming $\epsilon = \epsilon_{sat}$, we may take τ from Eq. (28). The result is

$$k_o L_d = \frac{2}{\epsilon} \frac{\alpha_o}{\alpha_2} \left(\frac{\omega_o}{\omega_p} \right)^3 . \tag{75}$$

If the acceleration length L is limited by L_d, Eqs. (62) and (66) give

$$\Delta\gamma = \epsilon L_d \omega_p / c \cos\theta . \tag{76}$$

Since $\cos\theta$ never differs greatly from unity, the last two equations give

$$\Delta\gamma = 2 \frac{\alpha_o}{\alpha_2} \frac{\omega_o^2}{\omega_p^2} . \tag{77}$$

Comparing this with the energy gain in the beat-wave accelerator [Eq. (21)], we see that

$$\frac{\Delta\gamma(\text{surf.})}{\Delta\gamma(\text{BWA})} = \frac{1}{\epsilon} \frac{\alpha_o}{\alpha_2} . \tag{78}$$

In colinear mixing, making $\alpha_o > \alpha_2$ would give the surfatron a greater advantage. In finite-angle mixing, we have shown that $\alpha_2 > \alpha_o$ is required. On the other hand, the fact that $\underline{k}_o$ is at an angle means that fresh light can be brought into the acceleration region. In any case, the energy gain of a surfatron is only $\approx \phi_{max}/\phi$ times larger than that of a BWA unless the bluer laser

beam can be replenished. It is claimed[11] that a further factor of 4 can be gained by optimizing the angle of the magnetic field rather than fixing it at 90°.

If $L = L_d$, then the acceleration time is $t = L_d/c$, and the position of the particles relative to the light pulse changes by $\delta\ell = (c - v_g)t$. Since $c - v_g \simeq (c/2)(\omega_p/\omega_o)^2$, Eq. (74) gives $\delta\ell/\ell = \alpha_o^2/4\varepsilon^2$. If, in addition, $\varepsilon = \varepsilon_{sat}$ as given by Eq. (24), we find

$$\frac{\delta\ell}{\ell} = \frac{3}{64}\frac{\alpha_o}{\alpha_2}\varepsilon \ll 1 . \qquad (79)$$

Thus the velocity mismatch in off-angle mixing does not cause the particles to outrun the light pulse within a depletion length.

7. Comparison of the surfatron and the BWA. The original attraction of the surfatron idea was its potential for unlimited acceleration; but we have seen in Eq. (78) that, when pump depletion is taken into account, the achievable energies differ by only a factor of a few. Ultra-high energies will require replenishing the pump in the surfatron or multi-staging of the BWA. Which will be easier will depend on the engineering design. On the other hand, the surfatron offers several other advantages over the BWA. First, it can be arranged to accelerate ions as well as electrons or positrons. Second, the spread in beam energy, $\Delta\gamma/\gamma$, is much smaller in the surfatron because all trapped particles converge to the same position on the plasma wavefront; this has been borne out by computation[6,8]. The spatial length of the bunches is also reduced. Third, there is some difference in synchrotron

radiation P. It was originally thought[10] that P was lower in the surfatron than in even a linear accelerator, because $\dot{\beta}$ was perpendicular to β. It has been pointed out[12], however, that for the same $\dot{\gamma}$ as a linear accelerator, the surfatron has the same P. A slight difference arises because in the BWA $\dot{\gamma}$ is not constant, while in the surfatron, $\dot{\gamma}$ is constant once the initial bounce oscillations have damped out. In neither case does P represent a serious loss. Finally, compared to the BWA the surfatron has some engineering problems involved with the dc magnetic field and the required width of the laser beam.

8. Comparison with vacuum schemes. It has long been known that electrons oscillating in a light wave will execute figure-8 orbits, and that these orbits will drift in the direction of $\underline{k}_o$ if the wave is not uniform. This drift, due to radiation pressure, cannot be used as an acceleration scheme because it is not only small but also disappears once the electron leaves the wave. Another proposal is to form a beat wave with two laser beams in a vacuum. Electrons or ions trapped in the beat wave envelope will be pushed toward the group velocity, which is c. If one calculates the equivalent electric field E_{eq} due to the ponderomotive force on an electron and compares that with the plasma wave field E_p at amplitude ϵ_{sat}, one finds that $E_{eq}/E_p \approx (3/16)^{1/3} (v_o/c)^{4/3}$, assuming $\alpha_o \approx \alpha_2$. Thus, for $v_o/c \approx 1$, these field are comparable. The problem is that the light wave E-fields are transverse and will transform to ≈ 0 in the wave (or particle) frame. A plasma is essential for converting $E_\perp$ into $E_{||}$, which does not transform away. Furthermore, because a plasma wave has

small group velocity, it serves as an energy storage device so that particles need not travel at exactly the velocity of the light pulse.

V. SIMULATIONS

The possibility of actually exciting a coherent plasma wave of finite width by optical mixing and of accelerating particles with it has been verified by 2D computer simulations[8,13]. These were done with a relativistic, electromagnetic code; the plasma was 60 × 60 c/ω_p in area with $T_i/T_e = 1$ and $M/m = 1836$; and the laser beams had frequencies $5\omega_p$ and $4\omega_p$, linear risetimes of $800/\omega_p$, a $\cos^2$ y profile, and peak intensity $v_o/c = 0.6$.

Simulations of the BWA show three separate focusing mechanisms working on the light waves, the plasma waves, and the accelerated beam. The laser light is initially self-focused by the relativistic effect: the oscillating electrons are heavier where the intensity is high, causing ω_p to be large and the index of refraction to be small on the axis. Later there is ponderomotive self-focusing as first the electrons and then the ions are pushed outwards by the ponderomotive force. The plasma waves, which also have their intensity peak on axis, have the same self-focusing mechanisms; for them, the ponderomotive force is relatively large[14]. The particle beam is also focused, in this case by the azimuthal magnetic field of its current. A return current flows in the plasma surrounding the acceleration region, and the

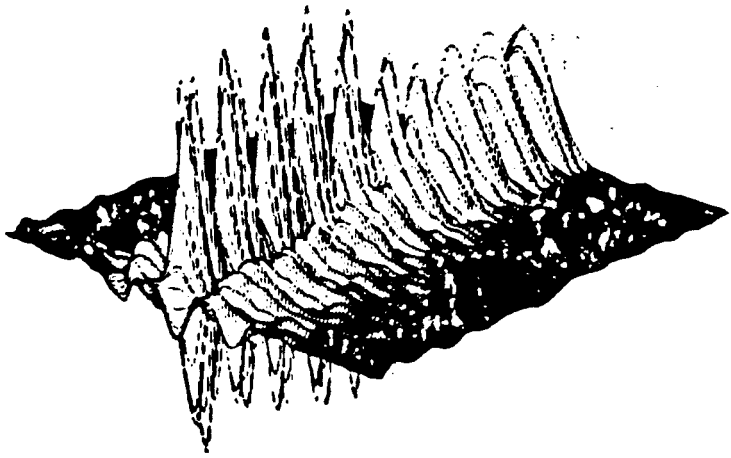

Fig. 10

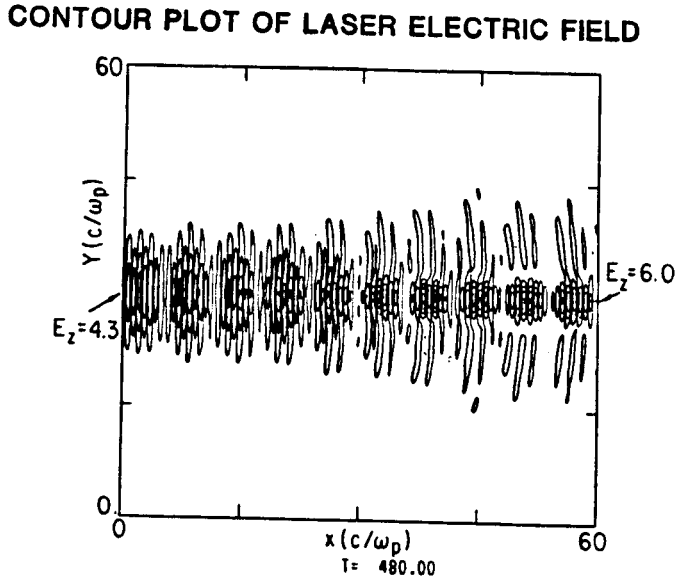
CONTOUR PLOT OF LASER ELECTRIC FIELD
60
0
0
60
Y(c/ω_p)
x(c/ω_p)
T= 480.00
E_z=4.3
E_z=6.0

Fig. 11

beam is driven inwards by the z-pinch effect.

Fig. 10 shows a 2D plot of the laser field, with the beams entering at the left, courtesy of W. Mori and colleagues[8]. Fig. 11 is the corresponding intensity contour plot. These show clearly the narrowing and intensifying of the light beam as it propagates into the plasma. Fig. 12 is a 2D plot of the plasma wave amplitude[13], and Fig. 13 a contour plot of this at a time when the right-hand portion has not yet been driven up to large amplitude. Though the waves are not pure sine waves and there is noise, the wavefronts are planar enough and coherent enough to trap and accelerate particles. The acceleration and focusing of the particle beam are shown in Fig. 14, which contains phase space plots, p_x vs x and p_x vs y, for two times. The p_x vs y plots show the trapping of electrons in the potential troughs and the increase in velocity with distance and time. The p_x vs y plots show that the fast particle radial distribution narrows in time due to the pinch effect.

Other simulations have verified the saturation level given by Eq. (24) and have shown the importance of beat wave excitation as contrasted with single-beam excitation of the forward Raman instability. In the latter case[13], other instabilities are much more easily excited at the same time as the one producing the desired wave: Raman backscatter and sidescatter, spontaneous magnetic field generation, self-focusing and filamentation, parametric decay, and the Weibel instability.

As for simulations of the surfatron effect, only a few runs with a dc magnetic field have been done so far[8,15]. These show the basic effect; but large particles energies have not yet been

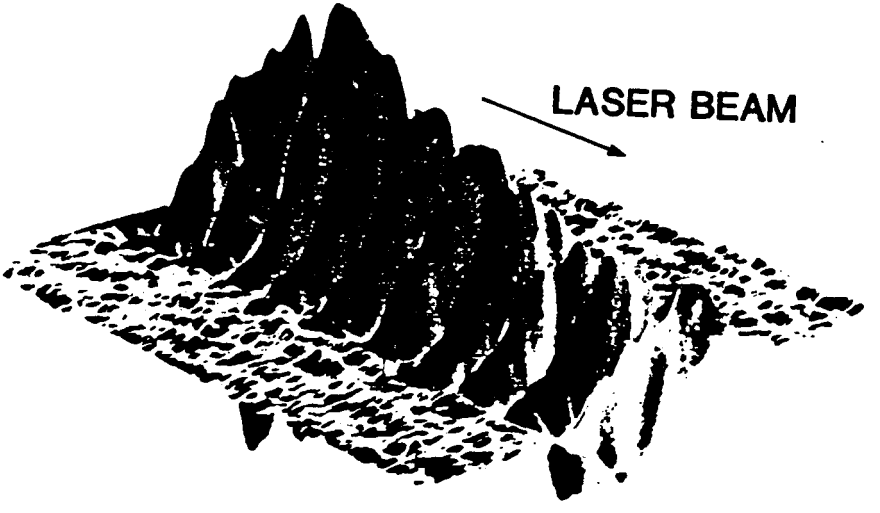
LASER BEAM

Fig. 12

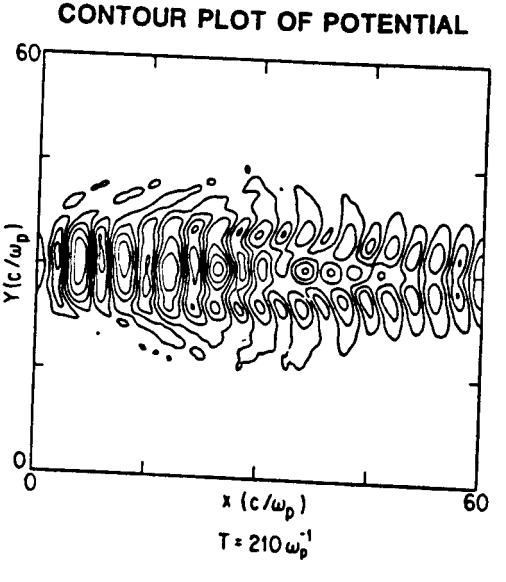
CONTOUR PLOT OF POTENTIAL
60
0
0
60
Y(c/ω_p)
x (c/ω_p)
T = 210 ω_p^-1

Fig. 13

PHASE SPACE PLOTS

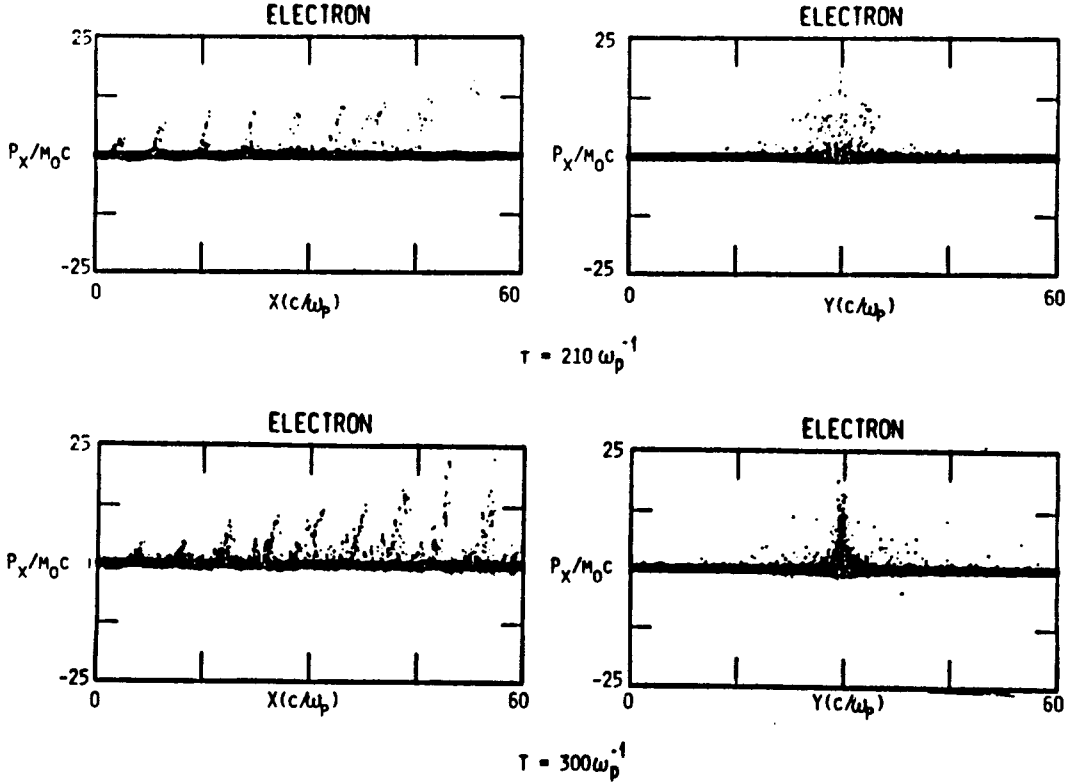

Fig. 14

seen, possibly because of the pump depletion phenomenon discussed above.

VI. EXPERIMENTS

The fundamental principles of beat wave excitation of plasma waves have already been verified experimentally. Optical mixing of co-propagating CO_2 laser beams was done by Joshi and Clayton[14] in the apparatus shown in Fig. 15. Beams of wavelength 10.26 and 9.55 μm are focused into an arc discharge plasma, and the light scattered past a beam block subtending a 5° half-angle is measured.

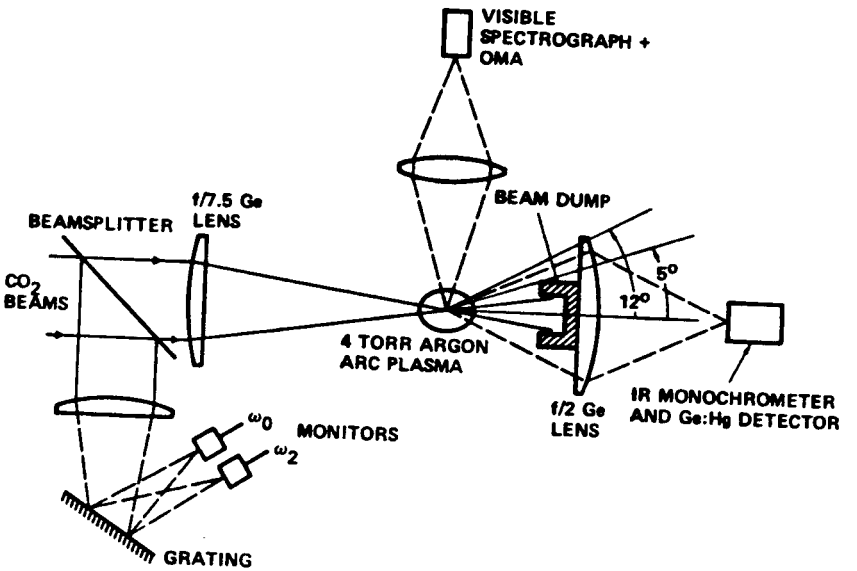

Fig. 15

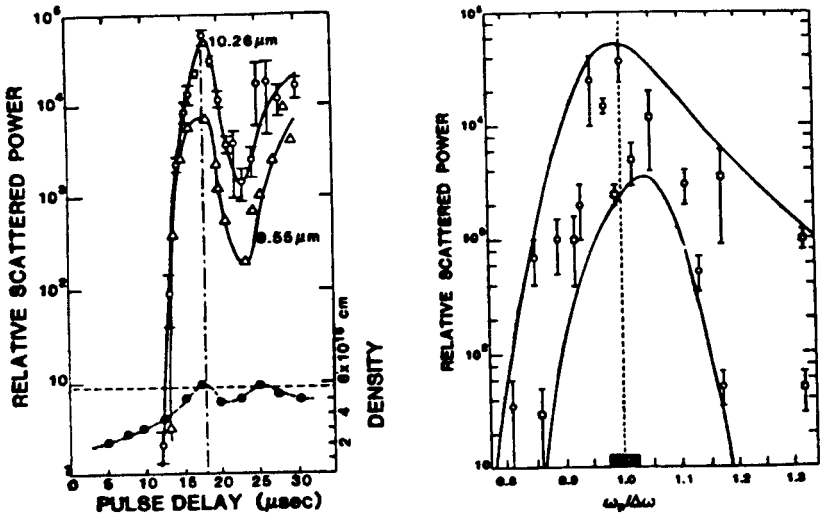
RELATIVE SCATTERED POWER
10.26μm
9.55μm
DENSITY
PULSE DELAY (μsec)
RELATIVE SCATTERED POWER

Fig. 16

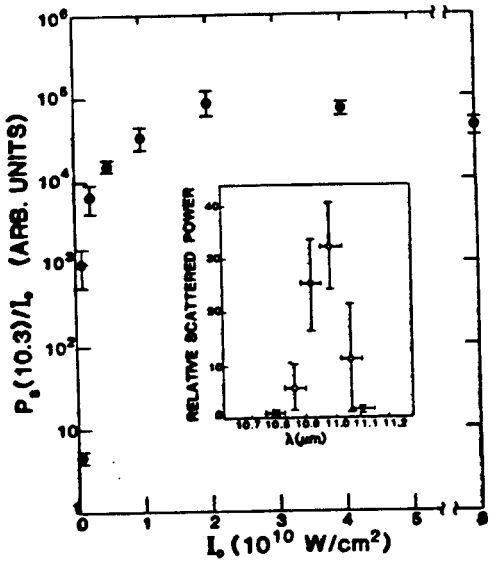
$P_s(10.3)/I_o$ (ARB. UNITS)
RELATIVE SCATTERED POWER
λ(μm)
I_o (10^{10} W/cm^2)

Fig. 17

When the resonance condition $\Delta\omega = \omega_p$ is satisfied, this light (which has no frequency shift) increases by a factor of 10^3, as shown in Fig. 16. This is interpreted as anomalous refraction caused by the ponderomotive force of the excited plasma wave. The latter is also detected by the 11-μm light created when it scatters the 10.26-μm beam. This feature is shown in Fig. 17 along with the growth curve, which shows a threshold below 10^9 W/cm^2.

Optical mixing of counter-propagating beams was done by Amini[16] in a theta-pinch plasma, which removes the complication of stimulated Brillouin scattering by virtue of having $T_i > T_e$. In this geometry, the value of k_p ($\approx 2k_o$) is large enough that the plasma wave can be measured directly by ruby-laser Thomson scattering at 8°. Fig. 18 shows the experimental arrangement, and Fig. 19 the scattered ruby spectrum with and without the CO_2 beams. The electron feature can be seen in the theta-pinch turbulence alone (top), thus giving a direct measurement of the plasma density. When the density is adjusted for $\omega_p = \Delta\omega$ and the CO_2 beams are turned on, the electron feature is enhanced by a factor of ≈70 (bottom). The scale to the right of the arrows has been changed to show the unshifted peak. The density resonance is shown in Fig. 20.

In the interval between the oral and written versions of this paper, these experiments at UCLA have been repeated with a higher intensity short pulse laser, and results with higher accuracy and new effects have been obtained.

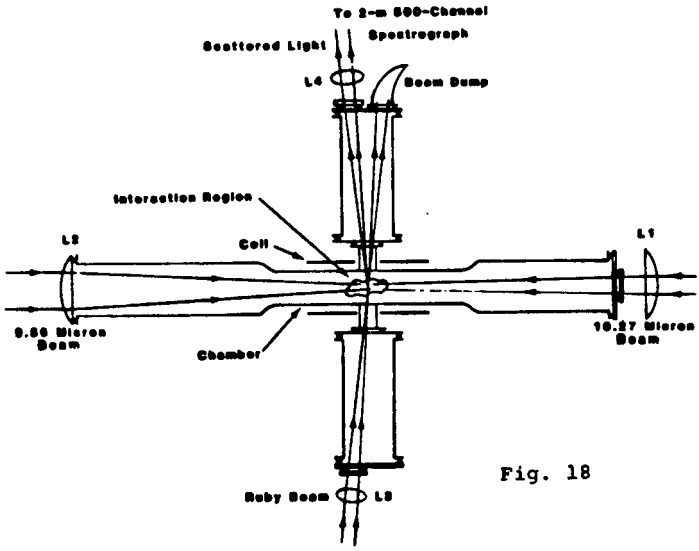

Fig. 18

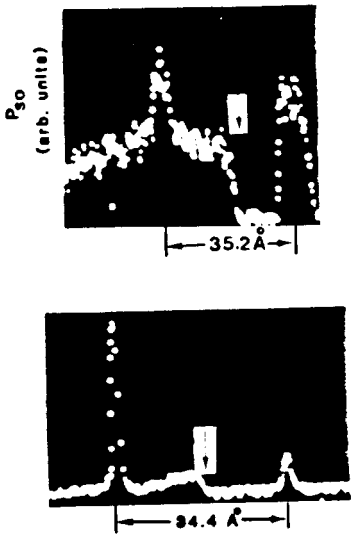

Fig. 19

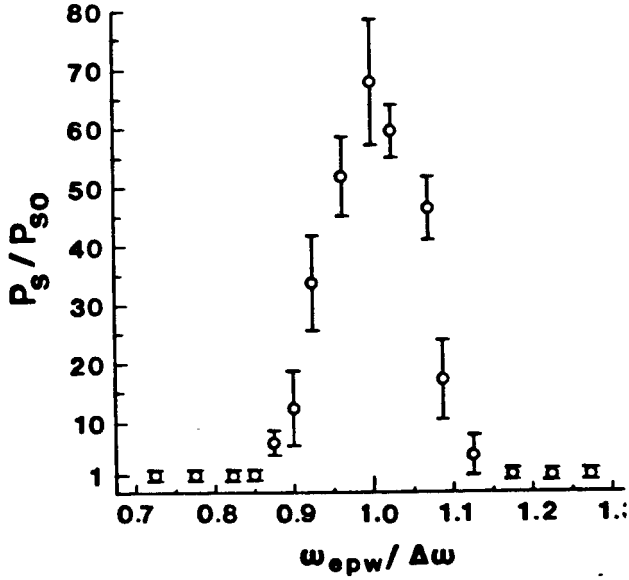

Fig. 20

VI. FUTURE INVESTIGATIONS

The first step in testing the feasibility of either the BWA or the surfatron is the investigation of laser excited plasma waves. That optical mixing in plasmas works has already been shown. It remains to see whether the saturation amplitude in a real experiment is limited by relativistic effects, as in Eq. (24), whether it can be driven past this value, or whether it is held below this value by some sort of nonlinear damping. Two-dimensional effects and plasma noise levels may also cause experiment to diverge from theory.

The production of intense laser pulses in the 10-50 psec regime is a technological problem that eventually has to be tackled. Short pulses are needed for several reasons. The time to reach ε_{sat}, shown in Fig. 3, is of this order of magnitude, and longer pulses not only waste energy but actually drive down the plasma wave when it gets out of phase. Secondly, the motion of ions must be avoided, since a change of density would destroy the carefully arranged resonance conditions. Third, the pulse length must be short compared with the growth rates of undesirable instabilities.

Instabilities can be grouped according to the driving mechanism. Those driven by the laser beams include filamentation, stimulated Brillouin scattering, and stimulated Raman backscatter and sidescatter. Filamentation requires the motion of ions over finite distances and is the easiest to avoid by short pulses. Brillouin scatter also arises on an ion time scale, but ions need only move half a laser wavelength. When SBS occurs, the ion

wave can reflect the incident beams, giving rise to a spectrum of undesired plasma modes.[17] This can be minimized by short pulsing, and by suitable choice of gas and temperature ratio. Raman scatter into other than the forward direction has a fast risetime but is more affected by Landau damping. To avoid SRS by the individual beams, it may be necessary to make them of equal intensity ($\alpha_o \approx \alpha_2$) so that the beat mode is preferentially excited. In that case, the wider beam in finite-angle mixing would require larger power.

There are also instabilities driven by the plasma waves themselves; for instance, resonant self-focusing[14] and parametric decay into an ion wave and another electron plasma wave. Both of these involve ion motions and should grow slowly. Finally, there are instabilities driven by the accelerated particle beam; for instance, kink instabilities and other z-pinch effects, and electromagnetic Weibel instabilities driven by electron anisotropy. How these are affected by the transverse de magnetic field in a surfatron is an interesting question. Though the present perception is that the growth times of instabilities are too long to be troublesome, only experimentation can show whether or not this view is correct.

The surfatron poses some interesting problems in gas discharge physics because the applied magnetic field is transverse to the axis. The production of a uniform, quiescent plasma which is long in the direction perpendicular to $\underline{B}$ has probably never been attempted. The simplest way would be to superimpose a $\underline{B}$-field on a rail-gap switch, as shown in Fig. 21. Rail gaps tend to arc in isolated spots rather than form a continuous sheet dis-

charge. This can be controlled by replacing the knife edge by a series of pins, each loaded with the same inductance. The device is then reminiscent of early TEA lasers, except that the plasma densities are much higher here. How uniform the density will be along the axis will depend on the rate of diffusion across $\underline{B}$. A second possible geometry might be that of an E-beam excited transverse-discharge laser, as shown in Fig. 22. The high-energy E-beam can travel along a magnetic field easily enough, but it will produce only a weakly ionized plasma. By focusing the light with cylindrical mirrors, it may be possible to cause a breakdown of the lasing gas along the axis, forming a long, uniform plasma.

In Fig. 23 we show a possible way to minimize the perturbing effect of the particle beam's magnetic field by making a surfatron with cylindrical symmetry. The dc field is created by a laser-target interaction. An auxiliary laser beam is focused onto a flat target supported by a spider mount. The blowoff plasma ejects the fast electrons which usually create a spontaneous magnetic field. Here, the fast electrons are collimated along the axis by a weak B-field created by an external coil, and the azimuthal spontaneous B-field is confined by a conducting cylinder (which also acts as a return path for the fast electron current). The beat-frequency laser beams are annular in cross section and enter around the target. They complete the ionization of the gas as in present experiments[14]. The plasma wave and accelerated beam are annular in cross section, and the surfing direction is radially inwards toward the axis. The B-field of the electron beam adds to the initial azimuthal field, so that the orbits have to be computed self-consistently; but $\underline{B}$ remains perpendicular to v_ϕ.

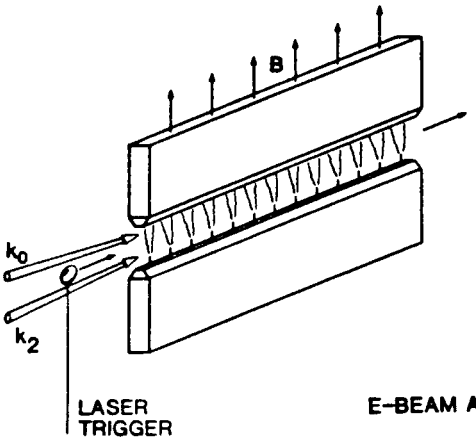

Fig. 21

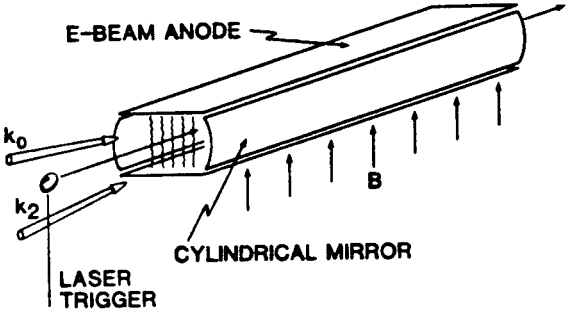

Fig. 22

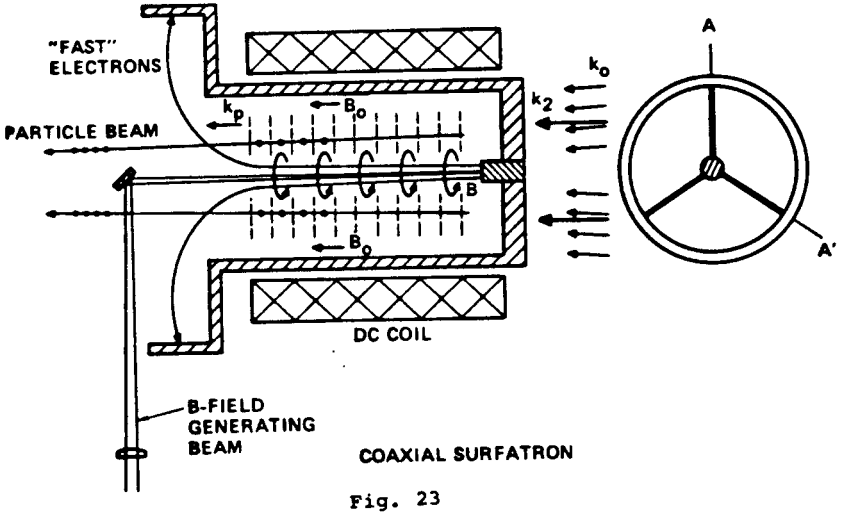

Fig. 23

When pump depletion is a problem, one could turn to a "waveguide" mode, as in Fig. 24. Plasma waves at an angle to the plasma axis are excited by two pairs of laser beams, $\omega_o - \omega_2 = \omega_p$ and $\omega_3 - \omega_4 = \omega_p$, such that $\omega_o - \omega_3 \neq n\omega_p$ and other mixing process are nonresonant. The plasma waves then add to produce an axial E-field, as in a $TM_{0,1}$ waveguide. This E-field accelerates particles along the axis, and the laser beams can be brought out of the plasma to be re-pumped, as shown in Fig. 5. The beams have to be reinjected in phase in each stage.

These ideas are only examples of the types of configurations that need to be studied once the plasma wave properties have been established. Beyond this, one can only conjecture about the actual accelerators that can be made. Let us take, for example, a plasma density n_o of 10^{18} cm^{-3}, corresponding to $E_{max} = 1$ GeV/cm $E = 100$ MeV/cm for $\epsilon = 0.1$. Suppose that a beam density $n_b = 0.1\ n_o$ is possible without perturbing the plasma wave too much, so that $n_b = 10^{17}$ cm^{-3}. Suppose further that the bunches in each potential trough have length $.01\ \lambda_p$, where $\lambda_p = 3.3 \times 10^{-3}$ cm. Then the number in each bunch is 3.3×10^{12} per cm^2; or, for a 1 mm^2 beam cross section, $N \approx 3 \times 10^{10}$. The current of the bunches passing at a frequency $f_p = 10^{13}$ Hz is $I = Nef_p = 48$ kA, giving rise to a 170-kG field at the beam edge. For colliding beams the luminosity would be $\approx (3.3 \times 10^{12})^2 \approx 10^{25}$ cm^{-2} sec^{-1}, provided that the repetition rate is ≈ 1 per sec on average. Since a 10-psec pulse contains 100 λ_p's, this would require the lasers to pulse at 10^{-2} Hz. These are all reasonable numbers, but the efficiency of the accelerator cannot compete with that of rf or microwave accel-

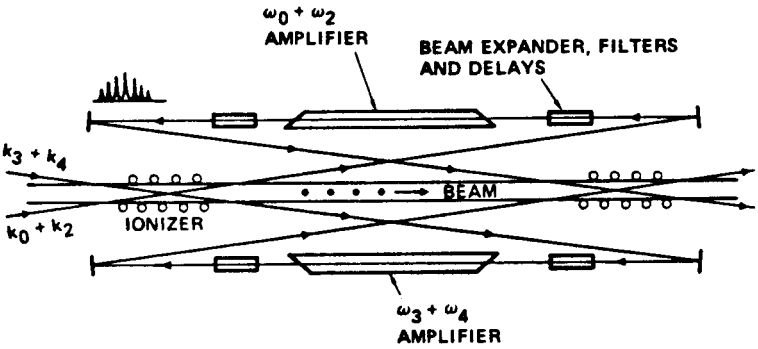

WAVEGUIDE MODE ACCELERATOR

Fig. 24

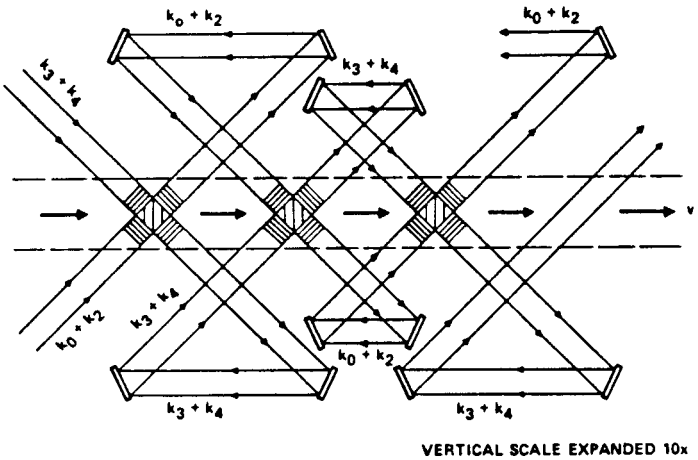

Fig. 25

erators because lasers are intrinsically inefficient. Simulations have shown[13] that as much as 15% of the laser energy can be converted to plasma waves and then to fast particles. If the lasers are 10% efficient, then the overall efficiency would be of order 1.5%.

The author wishes to thank Drs. T. Katsouleas and C. Joshi, Mr. W. Mori, and Prof. J. M. Dawson for helpful conversations in connection with this paper. This work was supported by U.S.D.O.E. contract DE-AT03-83ER40120 and National Science Foundation Grant ECS 83-10972.

REFERENCES

1. K. Estabrook and W. L. Kruer, Phys. Fluids 26, 1892 (1983).

2. C. Joshi, T. Tajima, J. M. Dawson, H. A. Baldis, and N. A. Ebrahim, Phys. Rev. Letters 47, 1285 (1981).

3. D. W. Phillion, D. L. Banner, E. M. Campbell, R. E. Turner, and K. Estabrook, Phys. Fluids 25, 1434 (1982).

4. T. Tajima and J. M. Dawson, Phys. Rev. Letters 43, 267 (1979).

5. J. M. Dawson, W. L. Kruer, and B. Rosen, in Dynamics of Ionized Gases, ed. by M. Lighthill, I. Inai, and H. Sato (University of Tokyo Press, 1973), pp. 47-61.

6. T. C. Katsouleas, Thesis, UCLA PPG-769 (1984).

7. M. N. Rosenbluth and C. S. Liu, Phys. Rev. Letters 29, 701 (1972).

8. C. Joshi, W. Mori, T. Katsouleas, J. M. Dawson, J. M. Kindel, and D. W. Forslund, Nature 311, 525 (1984).

9. J. M. Dawson, V. K. Decyk, R. W. Huff, I. Jechart, T. Katsouleas, J. N. Leboeuf, B. Lembege, R. M. Martinez, Y. Ohsawa, S. T. Ratliff, Phys. Rev. Letters 50, 1455 (1983).

10. T. Katsouleas and J. M. Dawson, Phys. Rev. Letters 51, 392 (1983).

11. R. Sugihara, S. Takeuchi, K. Sakai, and M. Matsumoto, Phys. Rev. Letters 52, 1500 (1984).

12. D. V. Neuffer, Phys. Rev. Letters 53, 1026 (1984).

13. D. W. Forslund, J. M. Kindel, W. B. Mori, C. Joshi, and J. M. Dawson, submitted to Phys. Rev. Letters (1984).

14. C. Joshi, C. E. Clayton, and F. F. Chen, Phys. Rev. Letters 48, 874 (1982).

15. D. J. Sullivan and M. M. Campbell, Bull. Amer. Phys. Soc. 29, 1176 (1984).

16. B. Amini and F. F. Chen, Phys. Rev. Letters 53, 1441 (1984).

17. H. C. Barr and F. F. Chen, Proceedings of the International Conference on Plasma Physics, Lausanne, Switzerland (1984), p. 66.